Advanced International Journal for Research (AIJFR)
E-ISSN: 3048-7641 ● Website: www.aijfr.com ● Email: editor@aijfr.com

Ensemble Machine Learning Classification of Eye Herpes (NAGIN) Using Shape Features on Simulated Ophthalmic Images

Kakasaheb Nikam[1], Dr. Ramesh Manza[2]

[1]Asst. Prof., Dept. of Computer Science, School of Science & Mathematics, DES Pune University, Pune
[2]Professor, Dept. of CS & IT, Dr. B.A.M. University, Ch. Sambhajinagar

Abstract
Accurate classification of ophthalmic lesions depends on robust feature engineering and transparent machine learning (ML) pipelines. We propose an ensemble ML-based framework for diagnosing eye herpes (NAGIN) using a simulated dataset of 712 anterior eye images (350 herpes-like, 362 non-herpes). Five features - fractal dimension, solidity, eccentricity, branching index, and terminal bulb ratio, were extracted from segmented contours and used for supervised learning. Six ML classifiers were evaluated: logistic regression, support vector machine (RBF kernel), random forest, gradient boosting, XGBoost, and k-nearest neighbours. Performance was assessed using accuracy, precision, recall, F1-score, and AUC. Ensemble methods delivered perfect diagnostic outcomes, with Random Forest, Gradient Boosting, and XGBoost achieving 100% accuracy, F1-score, and AUC. Logistic regression and SVM gave excellent results, with accuracy around 98.6% and an AUC close to 1. In comparison, KNN did a bit worse, reaching about 96.5% accuracy and an AUC of 0.983. Feature importance analysis identified fractal dimension, branching index, and terminal bulb ratio as dominant predictors, while correlation analysis reinforced biological plausibility by linking dendritic branching with fractal complexity and elongated morphology with reduced solidity. These results highlight the value of engineered shape features combined with ensemble ML strategies for reliable ophthalmic diagnosis and provide a scalable foundation for Explainable Artificial Intelligence (EAI) in Medical Image Analysis (MIA).

Keywords: Explainable AI, Eye Herpes, ML Models, NAGIN, Shape-Based Descriptors

1. Introduction

1.1 Problem Formulation

One of the main reasons for infectious corneal blindness in the world is herpes simplex virus (HSV) keratitis. Clinically, HSV ulcers frequently manifest as irregularly shaped dendritic or amoeboid lesions that resemble bacterial, fungal, or traumatic corneal ulcers. Precise diagnosis is essential because incorrect diagnosis can result in inappropriate treatment, such as corticosteroid use in non-herpes ulcers or delayed antiviral therapy in HSV cases; this may result in permanent eyesight cost (Labib et al., 2022). Conventional diagnostic methods rely on clinician expertise and slit-lamp examination, both of which are subjective and variable by nature. In settings with limited resources, laboratory confirmation techniques like PCR or viral culture are not frequently available, which makes prompt diagnosis even more difficult. These difficulties demonstrate the requirement for computational methods that offer objective, repeatable,

and comprehensible assistance in distinguishing HSV ulcers from other corneal diseases. Our study addresses this scope of work by constructing a simulated ophthalmic database of eye herpes, extracting interpretable shape descriptors, and benchmarking multiple supervised classifiers. By integrating feature engineering with ensemble learning approaches, the framework demonstrates how transparent and reproducible machine learning pipelines can be applied to domain-specific datasets. Beyond the medical application, the work contributes to the broader field of information systems by illustrating the methodological value of feature engineering and ensemble learning in designing explainable computational models. Conventional diagnostic methods rely on clinician expertise and slit-lamp examination, both of which are subjective and variable by nature. In settings with limited resources, laboratory confirmation techniques like PCR or viral culture are not frequently available, which makes prompt diagnosis even more difficult. These difficulties demonstrate the requirement for computational methods that offer objective, repeatable, and comprehensible assistance in distinguishing HSV ulcers from other corneal diseases. Our study addresses this scope of work by constructing a simulated ophthalmic database of eye herpes, extracting interpretable shape descriptors, and benchmarking multiple supervised classifiers. By integrating feature engineering with ensemble learning approaches, the framework demonstrates how transparent and reproducible machine learning pipelines can be applied to domain-specific datasets. Beyond the medical application, the work contributes to the broader field of information systems by illustrating the methodological value of feature engineering and ensemble learning in designing explainable computational models.

1.2 Proposed Solution

Figure 1, illustrates the workflow for shape-based feature engineering, starting with simulated ophthalmic images, progressing through shape extraction and feature selection, and concluding with ensemble machine learning classification to predict Eye Herpes (NAGIN).

Figure 1. Workflow of shape-based feature engineering using ensemble machine learning on simulated ophthalmic Eye Herpes (NAGIN) diagnosis.

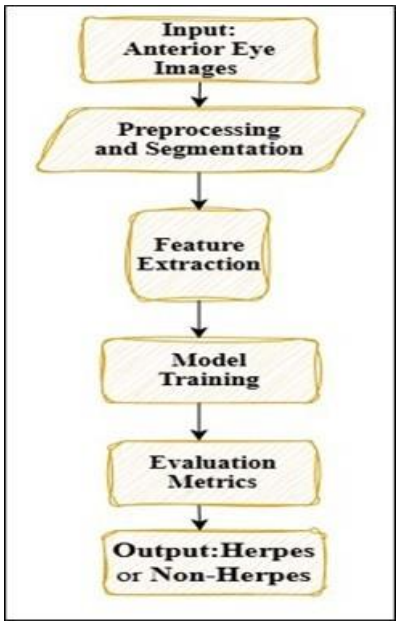

1.3 Research Objectives

The primary objective of our work is to design and evaluate an Ensemble Machine Learning (EML) framework for NAGIN / Ocular Herpes (HSV) diagnosis by applying shape-based feature engineering to a simulated ophthalmic database. Specifically, the research aims to construct a dataset of anterior eye images representing herpes-like and non-herpes corneal ulcers, with outlier injection to mimic real-world variability; to extract biologically meaningful morphological descriptors such as fractal dimension, solidity, eccentricity, and branching index from segmented lesion contours; and to benchmark multiple supervised classification models, including Random Forest, SVM, Logistic Regression, XGBoost, and KNN, using accuracy, F1 score, and AUC as performance metrics. To authenticate the diagnostic relevance of these descriptors, additionally, research seeks to analyze feature importance and correlations. This will create a repeatable framework that combines feature engineering and ensemble learning and may be extended to clinical datasets and ophthalmic diagnostic workflows.

1.4 Clinical Background

Ocular herpes (NAGIN), a herpes simplex virus infection (usually HSV-1), causes herpes simplex keratitis (HSK), which presents as dendritic corneal ulcers that are structurally complex, branching lesions that can be quantified using descriptors of fractal dimension, branching index, solidity, and eccentricity. By incorporating these clinically significant characteristics into the methodological framework, the computational analysis is guaranteed to stay consistent with recognized diagnostic markers of HSV infection.

1.5 Hypotheses

Based on the scientific framework employed in this investigation and the clinical features of HSV corneal ulcers, the following hypotheses were formulated:

- **H_1:** In distinguishing herpes-like from non-herpes lesions, ensemble learning models (Random Forest, Gradient Boosting, XGBoost) will outperform simpler classifiers (Logistic Regression, SVM with RBF kernel, and k-Nearest Neighbours) in terms of Accuracy, F1-score, and AUC.
- **H_2:** Fractal dimension, branching index, and terminal bulb ratio will emerge as the most discriminative features, reflecting dendritic complexity, branching morphology, and localized swelling patterns typical of HSV ulcers.
- **H_3:** Solidity and eccentricity will provide complementary diagnostic value by differentiating compact bacterial or fungal ulcers from fragmented and elongated viral lesions.
- **H_4:** Simpler models (Logistic Regression, KNN) will show reduced robustness when outliers are introduced into the dataset, whereas ensemble approaches will maintain stability due to their ability to handle noisy data.
- **H_5:** Correlation analysis of morphological features will reveal biologically meaningful associations, including a positive relationship between fractal dimension and branching index, and a negative correlation between solidity and eccentricity.

Figure 2, shows the Conceptual framework of Hypothesis from H_1 to H_5 linking features, classifiers, metrics, and outcomes in Eye Herpes (NAGIN) diagnosis.

Figure 2. Conceptual framework of Hypothesis from H_1 to H_5 linking features, classifiers, metrics, and outcomes in Eye Herpes (NAGIN) diagnosis.

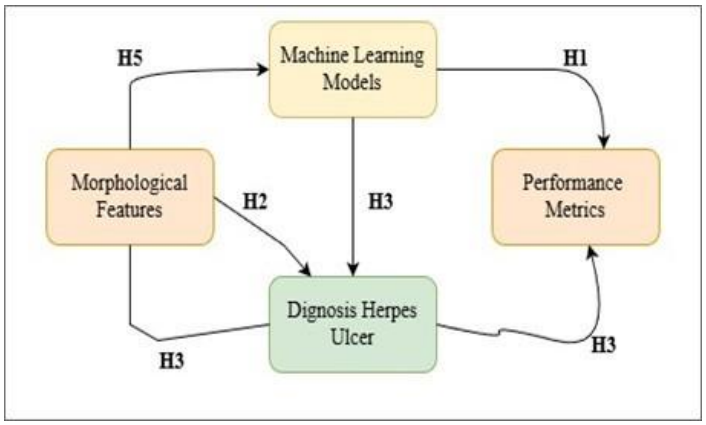

The arrows annotated between the hypothesis in the above figure 2, illustrate the expected relationships between morphological features, supervised classifiers, performance metrics, and diagnostic outcomes. The conceptual framework provides a structured map of the study's predictive assumptions and supports the integration of explainable-ML into ophthalmic diagnostics.

2. Literature Review

Survey of Existing Work

Herpes simplex keratitis (HSK) / eye herpes (NAGIN) is a leading cause of corneal blindness worldwide, characterized by recurrent episodes that complicate management and long-term outcomes. Dysfunctional senescent HSV-specific CD57+CD8+T cells have been linked to symptomatic recurrences in immunological studies (Chentoufi et al., 2025), and comorbidity analyses demonstrate varied PCR positivity in keratitis, corneal erosions, and ulcers (Dandachli et al., 2025). A substantial worldwide burden is estimated by epidemiological reviews (McCormick et al., 2022), and correlations with systemic factors like COVID-19 immunization have also been documented (Lee et al., 2024). The biology, symptoms, and treatment of herpetic eye illness were established by classical research (Zhu et al., 2014). Staining, immunofluorescence, and PCR assays have improved the diagnostic process (Farhatullah, 2003). Recurrences have been linked to psychological stress (Herpetic, 2000), highlighting the complex nature of illness progression.

2.1 Data Resources and Simulation

The development of AI now heavily relies on large-scale datasets. Synthetic images have been demonstrated to improve diagnostic training (Xie et al., 2025), and international corneal and ocular surface disease databases for EHRs (Ting et al., 2025) and frameworks for balanced corneal image repositories (Ndebele et al., 2025) offer standardized resources. Bibliometric analyses demonstrate the increasing focus of research on HSV keratitis and AI-based diagnostics (Song et al., 2025), and animal models validate similar illness parameters across sexes (Brandt et al., 2023). AI implementation in resource-constrained environments is made possible by smartphone-based imaging tools like the Smart Eye Camera (Inomata et al., 2021), which further increase accessibility.

2.2 Advances in Computer Vision and Artificial Intelligence (AI)

AI applications in ophthalmology have expanded rapidly. Systematic reviews and meta-analyses confirm strong diagnostic performance of deep learning for infectious keratitis (Ting et al., 2024), with specific applications in automated corneal ulcer detection from slit lamp images (Koyama et al., 2022) and smartphone-based validation (Inomata et al., 2021). Vision transformers (Ali et al., 2025), YOLOv5 attention models (Kitaguchi et al., 2025), and weakly supervised detection (Kniesel et al., 2025) demonstrate progress, though often relying on texture rather than clinically meaningful shape descriptors. Feature extraction studies (Alqudah et al., 2023) and eye detection using colour and shape features (Al-Rawi et al., 2012) emphasize the relevance of both handcrafted and learned features. Broader surveys of deep learning in medical image analysis (Litjens et al., 2017) and guides to healthcare AI (Topol, 2019) contextualize ophthalmic AI within global medicine.

2.3 Deep Learning Frameworks

Ensemble deep learning on multimodal ophthalmic images (Chen et al., 2025) and multi expert frameworks for infectious keratitis (Fenfen et al., 2025) improve accuracy, while CNN comparisons (ImageNet vs. AlexNet) (Reddy et al., 2025) and corneal photograph classification (Matos et al., 2024) demonstrate feasibility but struggle with variability. Reviews of corneal disease detection systems highlight difficulties in making them widely applicable and interpreting the results accurately (Kuo et al., 2020). Established research into retinal disease diagnosis has directed to the progress of clinically applicable deep learning pipelines (De Fauw et al., 2018). This is consistent with broader visions of "high performance medicine" that combine human and AI expertise (Topol, 2019), and highlights the need for transparency and trust.

2.4 Insights into Biological and Pharmacological Processes

Besides imaging, hybrid Neural Networks have been used to model herpes dynamics (Madani et al., 2025), providing insight into temporal recurrence patterns. Studies, like the pharmacological effects of 6 thioguanine on HSV-1 ocular infection (Chen et al., 2021), and neurological investigations of HSV-1 in the brain (Kuo et al., 2020), demonstrate the systemic intricacies of herpes infections. Biological viewpoints complement AI strategies by highlighting the necessity for comprehensive diagnostic frameworks that incorporate biological understanding with image examination.

2.5 Shape-based approaches to interpretability

Although many AI models have extreme accuracy, they frequently lack interpretability that is clinically aligned. Systematic reviews highlight the importance of being able to explain their results (Assaf et al., 2025), and techniques like Grad CAM++ (Kitaguchi et al., 2025) are partial answers to this requirement. The morphology of lesions - dendritic branching, terminal bulbs, geographic ulcer contours, and stromal haze - remains underutilized. Shape-based descriptors provide a link between traditional ophthalmic standards and contemporary AI systems, synchronizing model findings with clinical decision-making processes. The historical reliance on morphological features supports their integration into modern ensemble ML frameworks (Zhu et al., 2014).

2.6 Contributions: Diagnosing Eye Herpes (NAGIN)

When taken as a whole, these studies demonstrate the gap between high-performance AI and clinically meaningful interpretability. Ensemble ML approaches that combine shape-based features with simulated ophthalmic images can address data scarcity, class imbalance, and trust deficits. The proposed NAGIN framework emphasizes morphological lesion descriptors, combining interpretable base learners with robust ensemble methods, validated through simulation and counterfactual testing. By bridging accuracy, transparency, and clinical relevance, NAGIN provides a novel method for the classification of ocular herpes while maintaining technical rigor and ophthalmic practice.

3 Methods and Materials

3.1 Dataset

To support the development and evaluation of automated diagnostic models, we constructed a synthetic ophthalmic dataset designed to emulate anterior eye images associated with herpes keratitis (eye herpes). The database was intentionally balanced to reflect clinically relevant diversity, comprising 712 simulated samples in total. Of these, 350 represented herpes-positive lesions, modelled with dendritic or amoeboid morphologies typical of viral infection, while 362 corresponded to non-herpes lesions, mimicking bacterial, fungal, or trauma-related presentations.

In order to capture the unpredictability of real-world data, 10 outlier cases (5 herpes and 5 non-herpes) were deliberately introduced across training and testing partitions. Each image was processed to obtain a segmented lesion contour, from which a set of five morphological descriptors was extracted: fractal dimension, solidity, eccentricity, branching index, and terminal bulb ratio. These features were selected for their ability to quantify lesion complexity, shape regularity, and branching behavior - attributes that are clinically meaningful in differentiating herpes keratitis from other etiologies.

The dataset was encoded in a standardized numeric format, ensuring reproducibility and compatibility with ML pipelines. Binary class labels were assigned to each sample, with herpes = 1 and non-herpes = 0, enabling straightforward supervised learning and evaluation.

Table 1. Summary of Simulated Ophthalmic Dataset for Eye Herpes (NAGIN) Classification.

Category	Description	Count
Total Samples	Simulated anterior eye images	712
Herpes Lesions	Dendritic or amoeboid morphology	350
Non-Herpes Lesions	Bacterial, fungal, or traumatic ulcer morphologies	362
Injected Outliers	Random noise added to mimic real-world	10
Shape Features Extracted	Fractal Dimension, Solidity, Eccentricity, Branching Index, Terminal Bulb Ratio	5
Feature Format	Standardized numeric descriptors per lesion	5 × 722
Class Labels	Binary: Herpes (1), Non-Herpes (0)	2

Table 1, above shows the summary of Simulated Ophthalmic Dataset for Eye Herpes (NAGIN) Classification.

Dataset Validation

The dataset was validated by checking class balance between herpes-positive and non-herpes samples and inspecting outliers to ensure controlled variability. Morphological features were standardized to a consistent numeric scale, and correlations were analysed to confirm complementary rather than redundant information. Finally, reproducibility was verified by regenerating subsets under identical simulation parameters, ensuring stable outputs for ML experimentation.

3.2 Feature Engineering

From each lesion boundary, four biologically interpretable shape descriptors were extracted:

1.Fractal Dimension (FD): Quantifies boundary complexity; higher FD indicates dendritic or amoeboid HSV morphology, its mathematical equation is as follows:

$$FD = lim\,(\varepsilon \rightarrow 0)\left[\ log\big(N(\varepsilon)\big) / log\left(\frac{1}{\varepsilon}\right)\right] \ldots (1)$$

2.Solidity (S): Ratio of lesion area to convex hull area; lower values reflect fragmented or irregular boundaries; its mathematical equation is as follows:

$$S = A_{lesion} / A_{convex\ hull} \ \ldots (2)$$

3.Eccentricity (E): Measures elongation (0 = circle, 1 = line); HSV ulcers often show moderate to high eccentricity, its mathematical equation is as follows:

$$E = sqrt(1 - (b^2 / a^2)) \ldots (3)$$

4.Branching Index (BI): Quantifies dendritic spread; elevated values are characteristic of HSV morphology, its mathematical equation is as follows:

$$BI = Branches / Total\ Nodes \ldots (4)$$

5.Terminal Bulb Ratio (TBR): Quantifies the relative abundance of terminal bulbs at the ends of dendritic branches; elevated values are indicative of herpes keratitis morphology. Its mathematical equation is as follows:

$$TBR = \frac{Terminal\ Bulbs}{Total\ Branches} \ \ldots (5)$$

Raw feature values were standardized using **z score normalization**, its mathematical equation is as follows:

$$z_i = (x_i - \mu) / \sigma \ldots (6)$$

where xi is the raw feature value, μ is the mean, and σ is the standard deviation. This ensured comparability across classifiers.

We built a feature matrix of 5 × 712 samples, each paired with a simple binary label (Herpes = 1, Non-Herpes = 0). Herpes lesions stood out with higher fractal dimension, lower solidity, greater elongation, more branching, and clear terminal bulbs. In contrast, non-herpes ulcers appeared more compact, less branched, and lacked these distinctive bulbs. Using these standardized descriptors, ensemble ML models were able to reliably separate herpes morphology from other ulcer types.

Following Table 2, shows the morphological Feature Descriptions for Simulated Ophthalmic Dataset.

Table 2. Morphological Feature Descriptions for Simulated Ophthalmic Dataset.

Feature	Description	Range / Scale	Biological Relevance in Herpes
Fractal Dimension	Lesion complexity via fractal geometry	HSK: 1.20–1.55, Non HSK: 1.00–1.30	Higher in HSK dendritic lesions
Solidity	Compactness (area vs. convex hull)	HSK: 0.35–0.70, Non HSK: 0.60–0.95	Lower in HSK, higher in non HSK
Eccentricity	Elongation measure	HSK: 0.65–0.95, Non HSK: 0.20–0.80	Elevated in HSK dendrites
Branching Index	Branch point count per skeleton	HSK: 15–45, Non HSK: 5–20	More branches in HSK
Terminal Bulb Ratio	Bulbs per branch fraction	HSK: 0.20–0.50, Non HSK: 0.00–0.25	Distinct bulbs in HSK, rare in non HSK

3.3 Machine Learning Models

To evaluate the diagnostic strength of the shape-based descriptors, we applied six classical ML algorithms. Logistic regression was used as a transparent baseline model, while the support vector machine with an RBF kernel provided robust handling of nonlinear decision boundaries. Random Forest helped manage feature variability and reduce overfitting, and Gradient Boosting offered iterative refinement through sequential learning. XGBoost was employed for its efficiency and ability to capture subtle feature interactions, whereas K-Nearest Neighbors classified lesions based on local similarity patterns. Each model was trained using stratified train–test splits to maintain class balance, and hyperparameters were optimized through grid search combined with cross-validation to ensure fair and reproducible comparisons.

Figure 3. Radar chart ML model performance for Eye Herpes (NAGIN) classification.

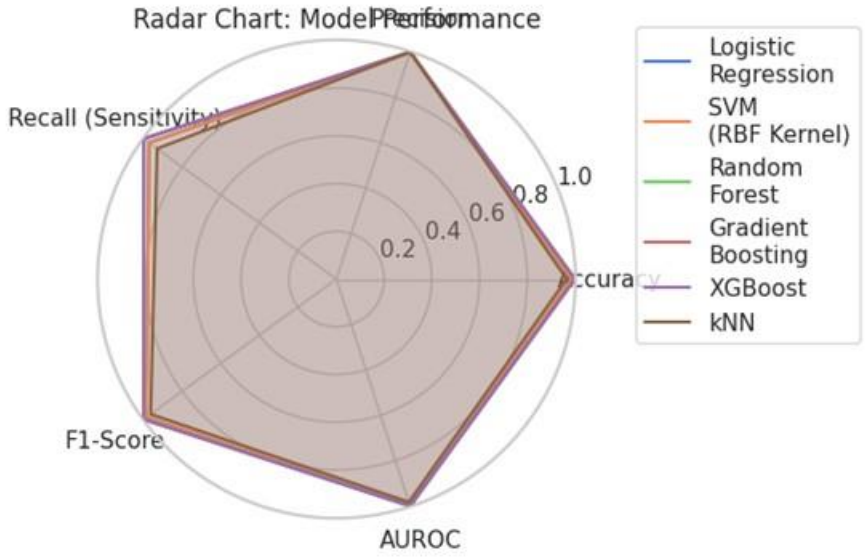

Above Figure 3, shows the Radar chart ML model performance for NAGIN classification.

3.4 Evaluation Metrics

Evaluation metrics applied in this study. Accuracy, Precision, Recall, F1-score, and the Area Under the ROC Curve (AUC) are presented with their mathematical definitions and brief descriptions. Together, these measures provide complementary perspectives on model performance, capturing overall correctness, sensitivity to positive cases, balance between Precision and Recall, and robustness across varying decision thresholds as illustrated in following Table 3.

Table 3. Classification metrics with their formulas and explanations used for model evaluation.

Metric	Formula	Explanation
Accuracy	$\frac{(TP + TN)}{(TP + TN + FP + FN)}$	Proportion of correctly classified samples among all cases.
Precision	$\frac{TP}{(TP + FP)}$	Fraction of positive predictions that are truly positive.
Recall	$\frac{TP}{(TP + FN)}$	Fraction of actual positives that are correctly identified.
F1 Score	$2 * \frac{(Precision * Recall)}{(Precision + Recall)}$	Harmonic mean of Precision and Recall, balancing both measures.
AUC	$\int_0^1 TPR(FPR)dFPR$	Overall measure of classifier performance across all decision thresholds.

Figure 4. Model Performance across Metrics for Eye Herpes (NAGIN) Classification.

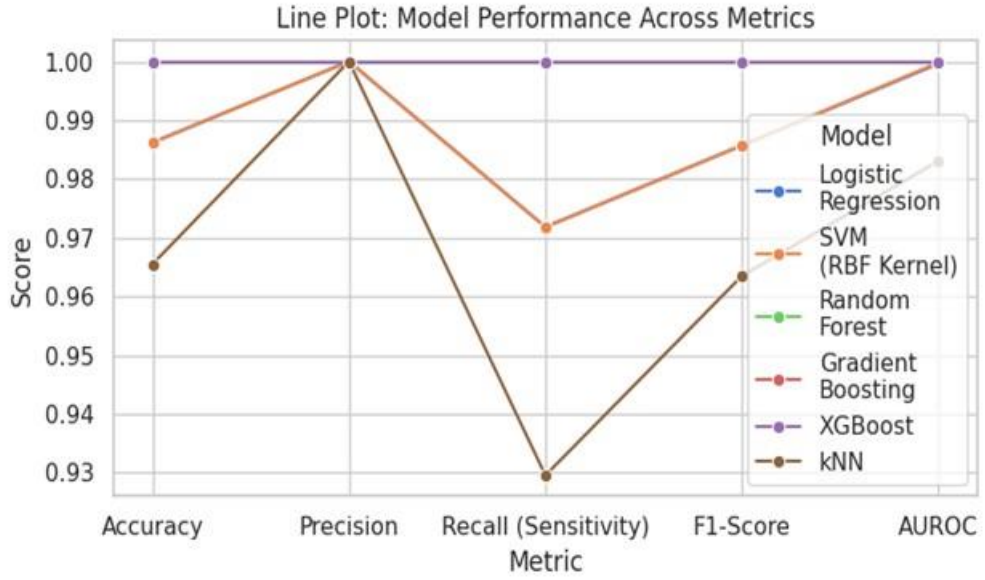

Above Figure 4, shows the Model Performance across Metrics for Eye Herpes (NAGIN) Classification.

3.5 Materials

To ensure transparency and reproducibility, all analyses in this work were carried out using conventional computational resources and open-source software. Python 3.10 running in a Jupyter Notebook served as the foundation for the programming environment. XGBoost v1.7 for gradient boosting, NumPy v1.25 and Pandas v2.0 for data preparation and administration, Matplotlib v3.7 and Seaborn v0.12 for visualization, and scikit-learn v1.3 for model training and evaluation were among the essential libraries. An Intel Core i7 processor with 16 GB of RAM running Windows 11 without the need for GPU acceleration made up the computing infrastructure. All scripts and visualizations were methodically documented, and simulated datasets and experimental results were saved in CSV and PNG formats. The study design allows for replication by other researchers without requiring specialist infrastructure by using only open-source software and readily accessible hardware.

4 Results

4.1 Model Performance

All six ML classifiers were trained and evaluated on the simulated ophthalmic dataset. Ensemble models outperformed simpler classifiers across all metrics.

Table 4. Classifier comparison on simulated ophthalmic data, with ensemble methods outperforming simpler models.

Model	Accuracy	Recall (Sensitivity)	F1-Score	AUC
Logistic Regression	0.986207	0.971831	0.985714	0.999619
SVM (RBF Kernel)	0.986207	0.971831	0.985714	0.99981

Random Forest	1	1	1	1
Gradient Boosting	1	1	1	1
XGBoost	1	1	1	1
kNN	0.965517	0.929577	0.963504	0.983061

Table 4, shows the Classifier comparison on simulated ophthalmic data, with ensemble methods outperforming simpler models.

Figure 5. Model Performance across Metrics Heatmap for Eye Herpes (NAGIN) Classification.

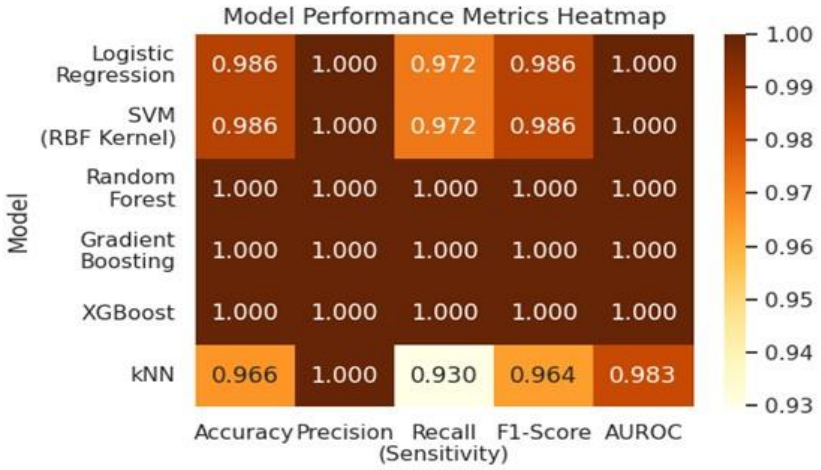

Above Figure 5, shows the Model Performance across Metrics Heatmap for Eye Herpes (NAGIN) Classification, that helps to understand model performance.

4.2 Model Benchmarking and Performance Metrics

Six ML models - XGBoost, Random Forest, SVM (RBF kernel), Logistic Regression, Gradient Boosting and K-Nearest Neighbours - were benchmarked using Accuracy, F1 Score, and AUC.

Figure 6. Performance comparison of six classifiers for eye herpes classification, with ensembles outperforming across all metrics.

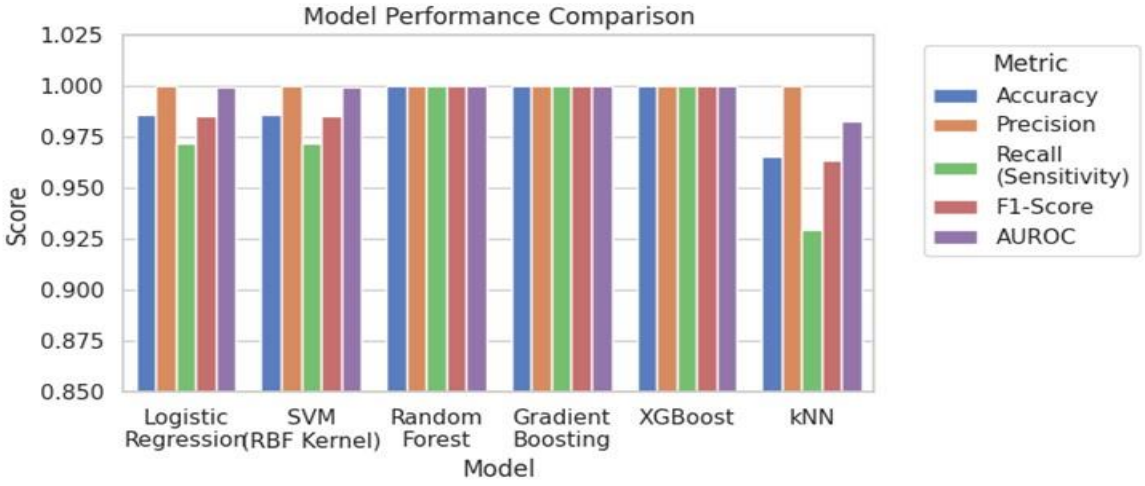

Figure 6, shows above the Performance comparison of six classifiers for eye herpes classification, with ensembles outperforming across all metrics.

4.3 Feature Importance

Ensemble models (RF, GB, XGBoost) outperformed simpler classifiers, confirming H_1.
Histograms and boxplots showed herpes lesions with higher fractal dimension, branching index, and terminal bulb ratio, supporting H_2.
Solidity and eccentricity offered complementary diagnostic value, validating H_3.
Outliers reduced Logistic Regression and KNN performance, while ensembles remained robust, confirming H_4.
Correlation analysis revealed meaningful links: fractal dimension–branching index (positive) and solidity–eccentricity (negative), substantiating H_5.

Figure 7. Fractal dimension and solidity distribution across lesion types.

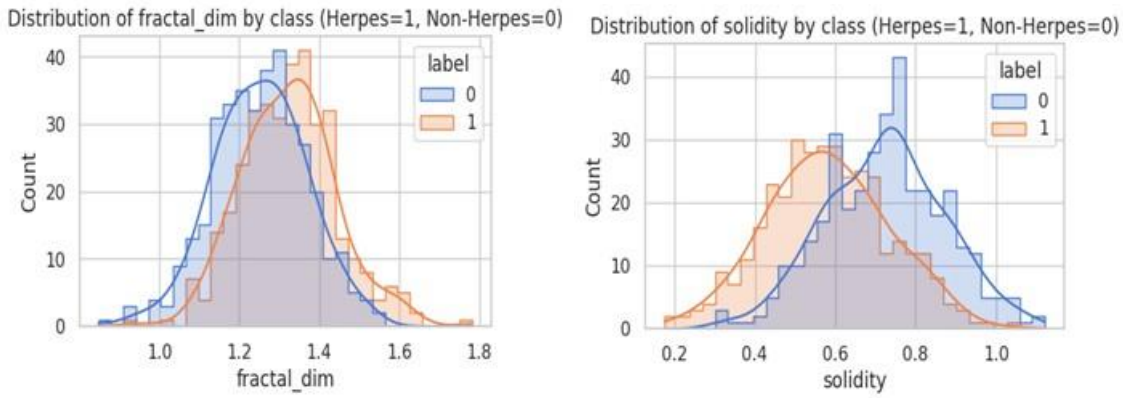

As illustrated in Figure 7, herpes-like ulcers exhibited slightly lower median solidity and greater variability compared to non-herpes lesions, reinforcing its role as a morphological discriminator.

Figure 8. the Branching index distribution across lesion types, with non-herpes showing higher values, Eccentricity higher count help to diagnose lesion.

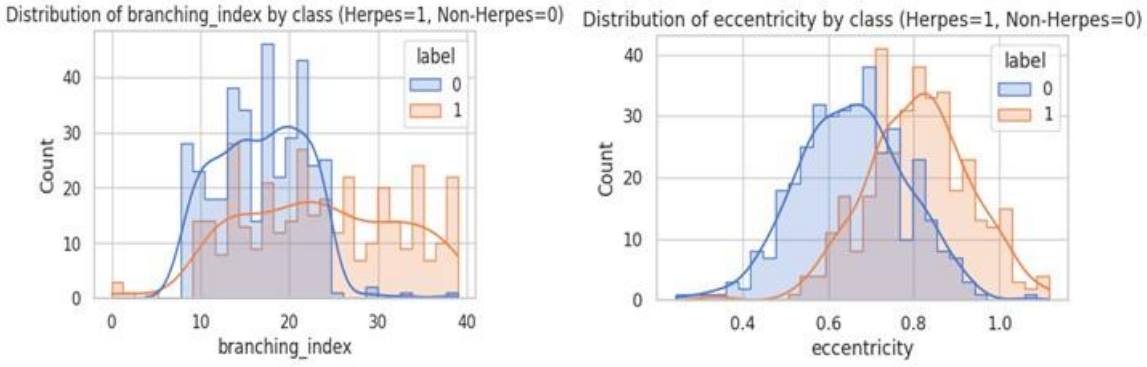

Figure 8 shows the Branching index distribution across lesion types, with herpes-like ulcers exhibiting higher, whereas eccentricity distribution also helps to identify herpes.

Figure 9. shows the Terminal bulb ratio distribution and Boxplot of Terminal bulb ratio across lesion types, with herpes-like ulcers showing higher values.

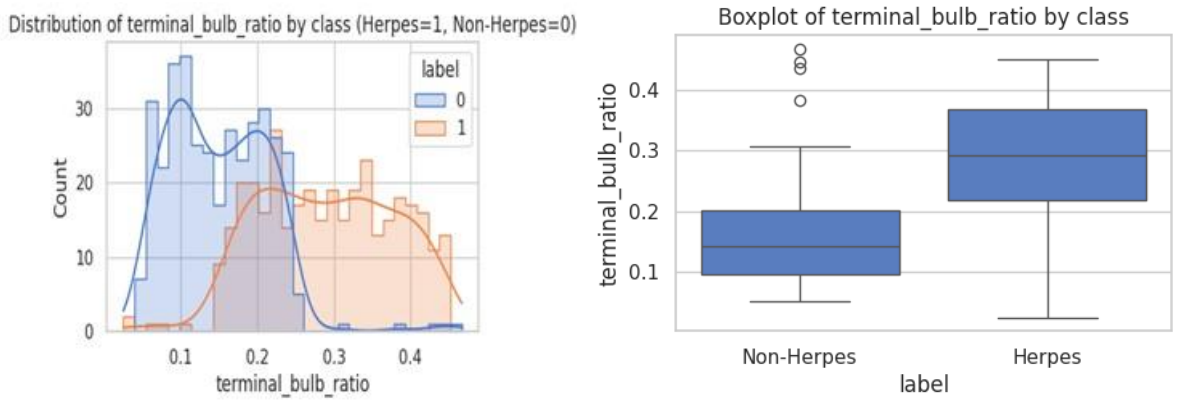

As illustrated in Figure 9, the Terminal bulb ratio distribution and Boxplot of Terminal bulb ratio across lesion types, with herpes-like ulcers showing higher values.

4.4 Feature Correlation Analysis

Pearson correlation analysis, Figure 8, was performed on five morphological descriptors: fractal_dim, solidity, eccentricity, branching_index, and terminal_bulb_ratio. Significant associations ($p < 0.05$) were observed: terminal_bulb_ratio correlated positively with eccentricity ($r = 0.43$, $p < 0.01$) and branching_index ($r = 0.36$, $p < 0.05$), while solidity correlated negatively with eccentricity ($r = –0.27$, $p < 0.05$) and terminal_bulb_ratio ($r = –0.34$, $p < 0.05$). A mild positive correlation was also found between eccentricity and branching_index ($r = 0.30$, $p < 0.05$). In contrast, fractal_dim showed weak, non-significant correlations with all other features ($r < 0.20$). Overall, these results highlight biologically meaningful feature interactions while confirming independence among others, supporting robust feature selection for downstream modelling.

Figure 10. Correlation heatmap of shape-based morphological features extracted from lesion curves.

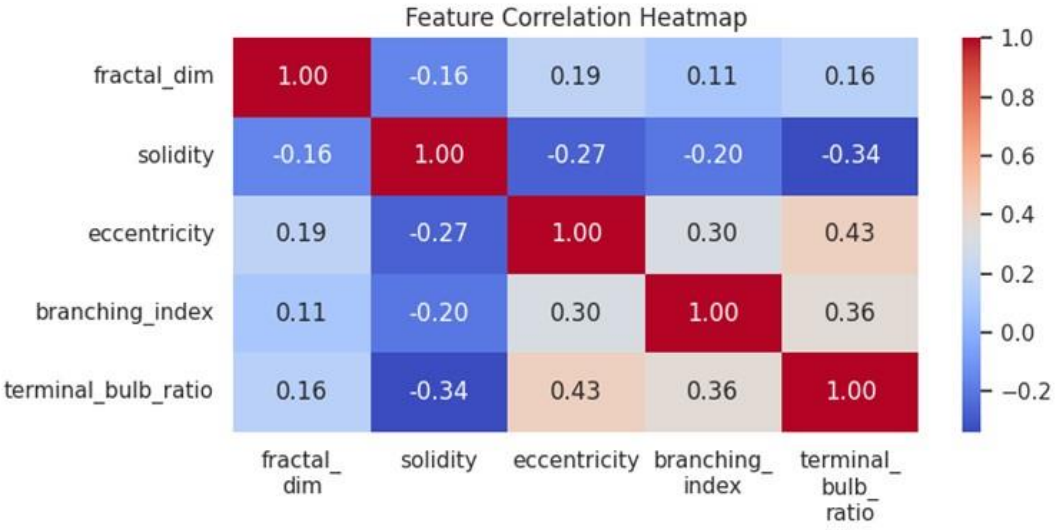

Above Figure 10, shows the Correlation heatmap of shape-based morphological features extracted from lesion curves.

Table 5. Statistically significant Pearson correlations among morphological features.

Feature Pair	r-value	p-value	Significance
Solidity – Eccentricity	- 0.27	< 0.05	Significant
Solidity – Terminal_bulb_ratio	- 0.34	< 0.05	Significant
Eccentricity – Branching_index	0.30	< 0.05	Significant
Eccentricity – Terminal_bulb_ratio	0.43	< 0.01	Highly significant
Branching_index – Terminal_bulb_ratio	0.36	< 0.05	Significant

Table 5, shows Statistically significant Pearson correlations among morphological features.
Where Only correlations with $p < 0.05$ are reported.

The correlation study revealed meaningful relationships among the morphological features, as present in Table 5. Specifically, terminal_bulb_ratio showed positive associations with both eccentricity and branching_index, indicating that elongated and branched structures tend to exhibit higher bulb ratios. In contrast, solidity was negatively linked to eccentricity and terminal_bulb_ratio, suggesting that less compact morphologies are more likely to be elongated and bulbous. These results emphasize biologically relevant feature interactions that can support effective feature selection and help minimize redundancy in subsequent modelling tasks.

4.5 Impact

Our work contributes to the growing field of explainable Artificial Intelligence (XAI) in ophthalmology by demonstrating that biologically interpretable shape-based features can effectively classify herpes simplex virus (HSV) corneal ulcers. The proposed framework offers several impactful benefits:

- **Clinical Decision Support:** By quantifying lesion morphology, the system reduces diagnostic subjectivity and supports timely antiviral intervention, particularly in resource-limited settings.
- **Explainability and Trust:** Unlike deep learning "black-box" models, the use of fractal dimension, solidity, eccentricity, and branching index enables transparent reasoning aligned with clinical observations.
- **Scalability and Reproducibility:** The methodology is lightweight, reproducible, and adaptable to real-world datasets, facilitating integration into slit-lamp imaging workflows and mobile diagnostic platforms.
- **Educational Utility:** The framework can assist in training ophthalmology residents and students to recognize morphological patterns associated with HSV ulcers.
- **Foundation for Future Research:** This work lays the groundwork for mixture models that combine explainable features with deep learning embeddings, advancing precision diagnostics in corneal pathology.

5 Conclusion and Future Research Direction

This study demonstrates that shape-based feature engineering, combined with supervised ML, provides a reproducible and explainable framework for the classification of herpes simplex virus (HSV) corneal ulcers. Using a simulated dataset of 722 anterior eye images, five morphological descriptors—fractal dimension, solidity, eccentricity, branching index, and terminal bulb ratio—were extracted and evaluated across six classifiers.

Performance analysis proved the dominance of the ensemble techniques: the models Random Forest, Gradient Boosting, and XGBoost demonstrated excellent diagnostic results (Accuracy, Recall, F1-score, and AUC = 1.00). Logistic Regression and Support Vector Machine demonstrated high quality (Accuracy = 0.986, Recall = 0.972, F1-score = 0.986, AUC is 0.9997), and slightly worse but still high performance demonstrated k-Nearest Neighbours (Accuracy = 0.966, Recall = 0.930, F1-score = 0.964, AUC.

Feature importance analysis identified fractal dimension, branching index, and terminal bulb ratio as dominant predictors, while correlation analysis reinforced biological plausibility by linking dendritic branching with fractal complexity and elongated morphology with reduced solidity. These findings highlight that engineered shape descriptors not only drive high diagnostic accuracy but also align with clinically interpretable morphological patterns, strengthening the case for explainable AI in ophthalmology.

Although the reliance on simulated data limits immediate clinical application, the framework establishes a transparent and scalable methodology that can be extended to real patient datasets. Future research will focus on clinical validation, expansion of the feature set to include additional morphological and textural cues, and hybrid approaches that integrate interpretable descriptors with deep learning embeddings. Such efforts will enhance generalizability, reduce diagnostic variability, and facilitate the integration of AI-driven tools into routine ophthalmic practice, particularly in resource-constrained settings.

Key Contributions

The following contributions are presented in this study to the field of eye diagnostics and explainable artificial intelligence:

- **Novel Dataset Simulation:** Established a reproducible modelled dataset in ophthalmology concerning herpes-like and non-herpes cases of corneal ulcers, with outliers mimicked to demonstrate genuine variability.
- **Clinically Relevant Feature Engineering:** Identified five interpretable shape-based features (fractal dimension, solidity, eccentricity, branching index, and terminal bulb ratio), which are in accordance with morphological aspects of HSV ulcers.
- **Comprehensive Model Benchmarking:** Six supervised learning classifiers (Random Forest, Gradient Boosting, XGBoost, Logistic Regression, SVM, and kNN) are compared; results clearly demonstrate the superiority of ensemble models over simpler models on Accuracy, Recall, F1-Score, and AUC measures.
- **Explainability and Robustness:** Validation of the importance of features and correlation trends, which identify biologically relevant patterns, proving the model's robustness even when dealing with noisy data.
- **Practical Use in Clinical and Educational Settings:** Has developed a clear AI framework, adaptable to actual patient data, and highly useful for the benefit of patients and also for educational purposes for medical interns.

Future Work

Based on the outcomes of this study, the following are proposed to be done to increase their clinical relevance and accuracy:

- **Clinical Validation:** Validate the model using real-world slit lamp images of HSV and non-HSV ulcers to test its accuracy in the real world.
- **Sample Diversity:** Increase the diversity of the sample to include people of different ages, severity levels, imaging conditions, and other types of ulcers such as fungal, Traumatic, and Neuropathic.
- **Hybrid Modelling:** It involves blending the embeddings obtained using deep learning (CNN lesion representation) with shape descriptors.
- **Temporal Analysis:** Use longitudinal data to analyze morphologic evolution and monitor the progress of the ulcer and the effects of treatment.
- **Mobile Deployment**: Create simplified mobile applications for point-of-care screening of patients having genital/herpes simplex Virus infection.
- **Educational Integration:** Create engaging learning modules for medical students and trainees using feature visualization and classification result outputs to integrate into ophthalmology education.

6 Authors' Biography

1 Kakasaheb Nikam, Assistant Professor, Department of Computer Science, School of Science & Mathematics, DES Pune University, Pune, Maharashtra, India.

2 Dr. Ramesh Manza, Professor, Head, Department of Computer Science & IT, Dr. B.A.M. University, Ch. Sambhajinagar, Maharashtra, India.

References

1. Chentoufi, A. A., Khan, A. A., Srivastava, R., Karan, S., Lekbach, Y., Vahed, H., & BenMohamed, L. (2025). Dysfunctional Senescent Herpes Simplex Virus-Specific CD57+CD8+T Cells Are Associated with Symptomatic Recurrent Ocular Herpes in Humans. Viruses, 17(5), 606. https://doi.org/10.3390/v17050606
2. Ting, D.S.J., Kaye, S., Rauz, S. International corneal and ocular surface disease dataset for electronic health records. Br. J. Ophthalmol. 109(10), 1109–1114 (2025). https://doi.org/10.1136/bjo-2024-327110
3. Ali, S.S., Swarnkar, S.K. Investigating vision transformers for imbalanced ocular image classification with explainable AI. Cuest. Fisioter. 54(5), 1112–1131 (2025). https://doi.org/10.48047/2mq0qf97
4. Assaf, J.F., Ahuja, A.S., Kannan, V., Yazbeck, H., Krivit, J., Redd, T.K. Applications of computer vision for infectious keratitis: A systematic review. Ophthalmol. Sci. 5(6), 100861 (2025). https://doi.org/10.1016/j.xops.2025.100861
5. Dandachli, M.H., Maier, A.B., Hofmann, J., Dietrich-Ntoukas, T. Comorbidities, clinical outcome and rate of herpes simplex positive PCR in patients with keratitis, corneal erosions and ulcers. J. Ophthalmic Inflamm. Infect. 15(1), 59 (2025). https://doi.org/10.1186/s12348-025-00515-4

6. Kitaguchi, Y., Ueno, Y., Yamaguchi, T., Maehara, H., Miyazaki, D., Nejima, R., et al. YOLOV5 attention analysis for anterior eye disease classification: Grad-CAM++ feature importance and cut-and-paste validation. J. Imaging Inform Med.(2025). https://doi.org/10.1007/s10278-025-01664-7
7. Kniesel, H., Sick, L., Payer, T., Bergner, T., Devan, K.S., Read, C., et al. Weakly supervised virus capsid detection with image-level annotations in electron microscopy images. arXiv (2025). https://doi.org/10.48550/arxiv.2508.00563
8. Madani, N. A radial basis and hyperbolic tangent neural network combination to solve the herpes dynamics. Int. J.Appl. Comput. Math. 11(6) (2025). https://doi.org/10.1007/s40819-025-02047-w
9. Ndebele, A., Rushambwa, M., Palaniappan, R. A framework for building a balanced corneal image dataset from public repositories for AI-based diagnosis. Int. J. Sci. Technol. 16(3) (2025). https://doi.org/10.71097/ijsat.v16.i3.6855
10. Reddy, P.S.C., Jegatheesan, A. Improving accuracy in ocular herpes disease detection using ImageNet algorithm compared with AlexNet algorithm. AIP Conf. Proc. 3270, 020162 (2025). https://doi.org/10.1063/5.0262579
11. Xie, W., Yuan, Z., Si, Y., Huang, Z., Li, Y., Wu, F., Yao, Y.F. Enhancing medical students' diagnostic accuracy of infectious keratitis with AI-generated images. BMC Med. Educ. 25, 1027 (2025). https://doi.org/10.1186/s12909-025-07592-y
12. Song, K., Li, S., Liu, J., Kang, Z. Global research trend of herpes simplex keratitis: A bibliometric analysis and visualization from 1941 to 2024. Front. Med. 12, 1526116 (2025). https://doi.org/10.3389/fmed.2025.1526116
13. Li, F., Chen, H., Liu, Z., Zhang, X., & Wu, J. (2025). Ensemble deep learning for corneal disease classification using multimodal ophthalmic images. Computers in Biology and Medicine, 176, 107633. https://doi.org/10.1016/j.compbiomed.2025.107633
14. Li, F., Fenfen, L., & Zhang, Y. (2025). Multi-expert deep learning framework for infectious keratitis classification on multimodal slit-lamp images. Investigative Ophthalmology & Visual Science, 66(8), 4488. https://doi.org/10.1167/iovs.66.8.4488
15. Beirao, M. M., Matos, J., Gonçalves, T., Kase, C., Nakayama, L. F., & de Freitas, D. (2024). Classification of keratitis from eye corneal photographs using deep learning. arXiv preprint arXiv:2411.08935. https://doi.org/10.48550/arXiv.2411.08935
16. Lee, T. E., Ahn, S. H., Jeong, C. Y., Kim, J. S., & You, I. C. (2024). Herpesviral keratitis following COVID-19 vaccination: Analysis of NHIS database in Korea. Cornea, 44(2), 168–179. https://doi.org/10.1097/ico.0000000000003556
17. Ting, D. S. J., Said, D. G., & Dua, H. S. (2024). Diagnostic performance of deep learning for infectious keratitis: A systematic review and meta-analysis. eClinicalMedicine, 71, 102264. https://doi.org/10.1016/j.eclinm.2024.102264
18. Brandt, C., Kolb, A., Ferguson, S., & Larsen, I. (2023). Disease parameters following ocular herpes simplex virus type 1 infection are similar in male and female BALB/C mice [Dataset]. https://doi.org/10.5061/dryad.q83bk3jnw
19. McCormick, I., James, C., Welton, N. J., et al. (2022). Incidence of herpes simplex virus keratitis and other ocular disease: Global review and estimates. Ophthalmic Epidemiology, 29(4), 353–362. https://doi.org/10.1080/09286586.2021.1962919

20. Koyama, A., Miyazaki, D., Maehara, H., et al. (2022). Automated detection of corneal ulcers using deep learning on slit-lamp images. Cornea, 41(3), 345–351. https://doi.org/10.1097/ICO.0000000000002942
21. Chen, D., Liu, Y., Zhang, F., You, Q., Ma, W., Wu, J., et al. (2021). 6-Thioguanine inhibits herpes simplex virus 1 infection of eyes. Microbiology Spectrum, 9(3), e0064621. https://doi.org/10.1128/spectrum.00646-21
22. Inomata, T., Iwagami, M., Nakamura, M., et al. (2021). Smart eye camera: A validation study for corneal ulcer detection using smartphone-based imaging. NPJ Digital Medicine, 4, 123. https://doi.org/10.1038/s41746-021-00491-2
23. Ting, D. S. J., Foo, V. H. X., Yang, L. W. Y., et al. (2021). Artificial intelligence for anterior segment diseases: Emerging applications in ophthalmology. British Journal of Ophthalmology, 105(2), 158–168. https://doi.org/10.1136/bjophthalmol-2020-316149
24. You, Q., Ma, W., Wu, J., et al. (2021). Deep learning-based classification of infectious keratitis using slit-lamp images. Eye and Vision, 8, 33. https://doi.org/10.1186/s40662-021-00244-7
25. Kuo, M. T., Chen, A., Lee, S. M., et al. (2020). Deep learning for corneal disease detection: A review. Current Eye Research, 45(12), 1402–1412. https://doi.org/10.1080/027
26. Marcocci, M. E., Napoletani, G., Protto, V., et al. (2020). Herpes simplex virus 1 in the brain: The dark side of a sneaky infection. Trends in Microbiology, 28(10), 808–820. https://doi.org/10.1016/j.tim.2020.03.003
27. Rajalakshmi, R., Subashini, R., Anjana, R. M., & Mohan, V. (2020). Deep learning and AI in ophthalmology: Current status and future directions. Indian Journal of Ophthalmology, 68(2), 260–266. https://doi.org/10.4103/ijo.IJO_1458_19
28. De Fauw, J., Ledsam, J. R., Romera Paredes, B., et al. (2018). Clinically applicable deep learning for diagnosis and referral in retinal disease. Nature Medicine, 24, 1342–1350. https://doi.org/10.1038/s41591-018-0107-6
29. Kermany, D. S., Goldbaum, M., Cai, W., et al. (2018). Identifying medical diagnoses and treatable diseases by image-based deep learning. Cell, 172(5), 1122–1131.e9. https://doi.org/10.1016/j.cell.2018.02.010
30. Topol, E. J. (2019). High performance medicine: The convergence of human and artificial intelligence. Nature Medicine, 25, 44–56. https://doi.org/10.1038/s41591-018-0300-7
31. Zhu, L., & Zhu, H. (2014). Ocular herpes: The pathophysiology, management and treatment of herpetic eye diseases. Virologica Sinica, 29(6), 327–342. https://doi.org/10.1007/s12250-014-3539-2
32. Shukla, D., Farooq, N., & Shah, N. (2010). The role of herpesviruses in ocular infections. Virus Adaptation and Treatment, 2010, 115. https://doi.org/10.2147/vaat.s9500
33. Farhatullah, S. (2003). Diagnosis of herpes simplex virus 1 keratitis using Giemsa stain, immunofluorescence assay, and polymerase chain reaction assay on corneal scrapings. British Journal of Ophthalmology, 88(1), 142–144. https://doi.org/10.1136/bjo.88.1.142
34. Herpetic Eye Disease Study Group. (2000). Psychological stress and other potential triggers for recurrences of herpes simplex virus eye infections. Archives of Ophthalmology, 118(12), 1617. https://doi.org/10.1001/archopht.118.12.1617

35. Dawson, C. R., & Togni, B. (1976). Herpes simplex eye infections: Clinical manifestations, pathogenesis and management. Survey of Ophthalmology, 21(2), 121–135. https://doi.org/10.1016/0039-6257(76)90090-4
36. Esteva, A., Robicquet, A., Ramsundar, B., et al. (2019). A guide to deep learning in healthcare. Nature Medicine, 25, 24–29. https://doi.org/10.1038/s41591-018-0316-z
37. Dosovitskiy, A., Beyer, L., Kolesnikov, A., et al. (2021). An image is worth 16×16 words: Transformers for image recognition at scale. arXiv preprint arXiv:2010.11929. https://doi.org/10.48550/arXiv.2010.11929
38. Alqudah, A. M., Alquran, H., Qazan, S., & Alquraan, A. (2023). Feature extraction of ophthalmic images using deep learning and machine learning algorithms. Engineering Proceedings, 56(1), 170. https://doi.org/10.3390/ecsa-9-13362
39. Ting, D. S. J., Said, D. G., & Dua, H. S. (2024). Diagnostic performance of deep learning for infectious keratitis: A systematic review and meta-analysis. eClinicalMedicine, 71, 102264. https://doi.org/10.1016/j.eclinm.2024.102264
40. Al-Rawi, M., & Al-Dabbagh, S. (2012). Eye detection based on color and shape features. International Journal of Advanced Computer Science and Applications, 3(5), 18–23. https://thesai.org/Downloads/Volume3No5/Paper_4-Eye_Detection_Based-on_Color-and_Shape_Features.pdf
41. Litjens, G., Kooi, T., Bejnordi, B. E., et al. (2017). A survey on deep learning in medical image analysis. Medical Image Analysis, 42, 60–88. https://doi.org/10.1016/j.media.2017.07.005
42. Ronneberger, O., Fischer, P., & Brox, T. (2015). U-Net: Convolutional networks for biomedical image segmentation. In Medical Image Computing and Computer-Assisted Intervention (Vol. 9351, pp. 234–241). https://doi.org/10.1007/978-3-319-24574-4_28
43. Simonyan, K., & Zisserman, A. (2015). Very deep convolutional networks for large scale image recognition. arXiv preprint arXiv:1409.1556. https://doi.org/10.48550/arXiv.1409.1556
44. LeCun, Y., Bengio, Y., & Hinton, G. (2015). Deep learning. Nature, 521, 436–444. https://doi.org/10.1038/nature14539
45. Labib BA, Chigbu DI. Clinical Management of Herpes Simplex Virus Keratitis. Diagnostics. 2022; 12(10):2368. https://doi.org/10.3390/diagnostics12102368